Maximum depth of magnetisation of Australia, its uncertainty, and implications for Curie depth

Richard Chopping [a,b,*], Brian L.N. Kennett [a]

[a] Research School of Earth Sciences, Australian National University, 142 Mills Rd, Acton, ACT 0200, Australia
[b] Resources Division, Geoscience Australia, GPO Box 378, Canberra, ACT 2601, Australia

ARTICLE INFO

ABSTRACT

The Curie depth is the depth at which the crust and uppermost mantle cease to be ferromagnetic or ferromagnetic, the main cause of crustal magnetism, due to the action of geothermal effects. One method to estimate the Curie depth for Australia is to map the base of magnetisation derived from observations of magnetic intensity. We have used a nonlinear direct sampling inverse technique to fully explore the parameter space of a fractal forward model of magnetisation. This produces an ensemble of models that allow us to produce maps of both the maximum depth of magnetisation and its uncertainty for Australia. The base of magnetisation varies significantly across the continent, between 10 and 70 km depth, with an uncertainty of 7–10 km. The variations in magnetisation depth conform with the boundaries of geological provinces due to their differing magnetic properties: In general, cratons and older provinces generally show a deeper base of magnetisation results and hence may be inferred to have deeper Curie depths, reflecting that these areas are on the whole cooler. We also find general agreement in our results with known geothermal anomalies.

1. Introduction

The Curie depth is the depth at which rocks cease to be ferri- or ferromagnetic because their temperatures are above their Curie point [1]. Note that within a region, temperatures increase with depth due to the local geothermal gradient and thus the Curie depth will reflect the local geothermal gradient. The Curie point of any rock depends on the Curie points of the individual minerals in the assemblage (Fig. 1: note that the Néel point is the corresponding temperature for ferrimagnetic or antiferromagnetic minerals). The Curie depth for an area, therefore, reflects both the local thermal regime and the mineralogy of the magnetic minerals within that area. Curie depth measures can provide estimates of the geothermal state away from drill holes and other direct observations. Variations in Curie depth can also provide information on the boundaries between different geological regions, either due to changes in mineralogy that produce changes in the Curie point and hence depth, or through different geothermal regimes in different geological regions. As magnetite is the most magnetic mineral, the Curie depth is often interpreted to reflect the depth to the temperature at which the Curie point of magnetite is reached,

approximately 580 °C [2]. Nevertheless, there is the potential for this Curie point to be lower; for instance, the addition of titanium to magnetite greatly reduces the Curie point (Fig. 1A).

In previous studies, the Curie depth, or a proxy for it, has been mapped using two main approaches ([3]):

a Calculations for an assumed mineralogy, based on temperature data which may be directly measured (from, e.g., drill hole temperature data) or inferred (from, e.g., seismic velocities); or
b Models from magnetic data to establish the base of magnetisation.

Of these approaches, magnetic methods are the most commonly used methods to estimate the Curie depth. Magnetic methods have been routinely applied to this problem for about 40 years and fall into two classes:

a Approaches using satellite magnetic data at scales up to global scale, e.g., [4]; and,
b Approaches using more local magnetic data, from ground or aeromagnetic magnetic intensity data (e.g., [1,5]).

Ultimately, both methods seek to establish the base of magnetisation as a proxy for Curie depth, as they assume that rocks beneath this depth are at a temperature above their Curie point.

* Corresponding author at: Research School of Earth Sciences, Australian National University, 142 Mills Rd, Acton, ACT 0200, Australia.
   E-mail address: richard.chopping@anu.edu.au (R. Chopping).
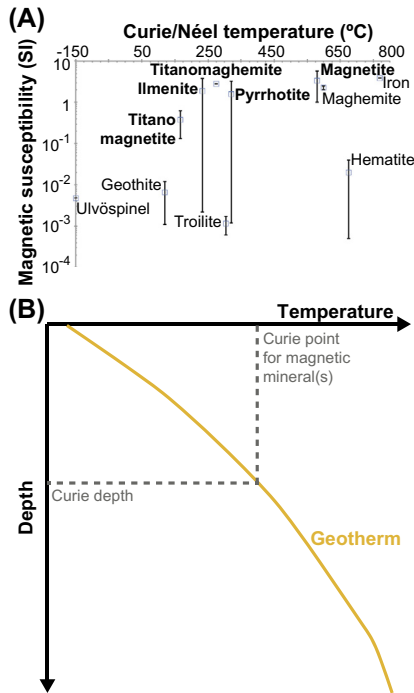
Fig. 1. (A) Relationship between magnetic susceptibility and Curie point for selected minerals (data after [2]). (B) Relationship between geothermal gradient and Curie depth, given a specific Curie point.

It is with this aim we have undertaken our study. Unfortunately, the base of a magnetic layer is the most difficult parameter to extract from the observations, as the signal of magnetic intensity falls off with the cube of distance [2], which means that magnetic methods are relatively depth-insensitive. This difficulty is enhanced when no knowledge of the magnetic properties of the region is available. There are also circumstances where the base of magnetisation may not fully reflect the Curie depth, for instance, in the case of geological environments where magnetic material may not be present at depths that correspond to the expected isotherm (such as 580 °C).

Modelling satellite magnetic data to define the base of magnetisation requires techniques that can handle relatively thin magnetic layers. Due to the large separation between the magnetic sensor (300 km altitude) and the depths of both the top and bottom of the magnetic layer (~5–50 km), the signals from the top and bottom of the magnetic layer are difficult to separate [6]. An example of the modelling techniques used for defining the Curie depth from satellite magnetic data is the approach taken by Fox Maule et al. [4] to determine the Curie depth, and hence the thermal structure, for Antarctica. This model solves for magnetic dipoles in individual cells to reproduce the observed magnetic field. The dipole for each cell is then used to solve for a magnetic layer with a constant magnetic susceptibility, with the depth to top fixed at the thickness of sediments from the 3SMAC model [7]. The magnetic base is allowed to vary until it either reproduces the magnetic dipole for the cell, or lies at the depth of the 3SMAC Moho. The assumption of constant susceptibility is a significant limitation of this methodology as magnetic susceptibilities of rocks can vary by several orders of magnitude [2].

Approaches using local magnetic data use models where the depth of the base of the magnetic layer is significantly deeper, in relation to the magnetic sensor, than the depth to the top of the layer [1]. Such techniques can be combined with satellite magnetic data to constrain the longest wavelength components. An example of this class of models is the use of a layer of random sources

employed by Spector and Grant [5]. In this study, a 1D radially-averaged power spectra which avoids complications from specific assumptions about the strength of magnetic susceptibilities within a region is used. Later techniques, e.g., [1,8], build upon [5] by either employing manual or semi-manual curve fitting of straight-line segments to the 1D power spectra, or automated inversions for fractal models of magnetisation. In all cases, the power spectra can either be used in a raw state or corrected for the effects of self-similarity through a scaling factor [1].

Apart from uncertainties due to the assumption of random equivalent sources confined to a layer, all the approaches to the estimation of the base of magnetisation tend to be limited in their accuracy because of the difficulty of specifying the longest wavelength components of the magnetic field. Such components are better controlled in satellite magnetic data, although aeromagnetic data that have been constrained by long-wavelength (>400 km) or satellite magnetic data can represent a useful compromise [1]. Additionally, any technique that windows data into individual tiles is limited to resolving a maximum depth of magnetisation of half of the window width [2], due to limitations on the accessible wavelengths. Practically, however, the window widths must be at least 4–5 times more than the expected maximum depth of magnetisation to adequately resolve appropriate wavelengths that allow imaging of the base of the magnetic sources [8]. This requirement limits the spatial resolution of all techniques to broad scales only, especially in areas that are expected to be relatively cold, which would result in a deeper depth to base of magnetisation and hence a deeper Curie depth than in warmer regions.

All the approaches employed for estimating the Curie depth depend to varying degrees on the implicit assumption that long wavelength features result from deep sources. However, such long wavelength features can also result from shallow yet spatially extensive sources [2]. This ambiguity adds to the uncertainty in the results for the depth to the base of magnetisation. Models based on self-similarity can handle relatively shallow, but wide, features with the use of a scale factor for the level of self-similarity [1,8].

Although many techniques have been employed to map the base of magnetisation and hence infer the Curie depth, discussions of the uncertainty in the results of these studies are rather limited. In principle, determining the base of a magnetic body is the most uncertain part of magnetic modelling [2], yet it is crucial to understanding to what extent such results can be interpreted. Understanding not just the Curie depth, but also its uncertainty, we feel is key to the applicability of these results.

1.1. Motivation and previous studies of the Australian Curie depth

Australia is a continent characterised by some of the oldest rocks and landscapes across the globe [9]. Tectonically, the continent is broadly divided into five main elements with a number of geological provinces contained within each of these elements. In many parts of the Australian continent outcrop of basement rocks is limited, with recent sedimentary basins and widespread regolith obscuring basement geology. Although the basement geology of the cover is obscured by this younger geology, many geological features interpreted to reflect basement geology are evident in the magnetic anomaly data available for Australia (Fig. 2).

Geothermally, Australia is also a continent of extremes ([13], and Fig. 3). The Archean cratons of Western Australia are characterised by particularly low geothermal gradients. In contrast, some of the Proterozoic rocks of Australia include granites with very high heat-production because they are rich in radiogenic elements. Such materials produce significant heat flow and elevated temperatures at depth [14].
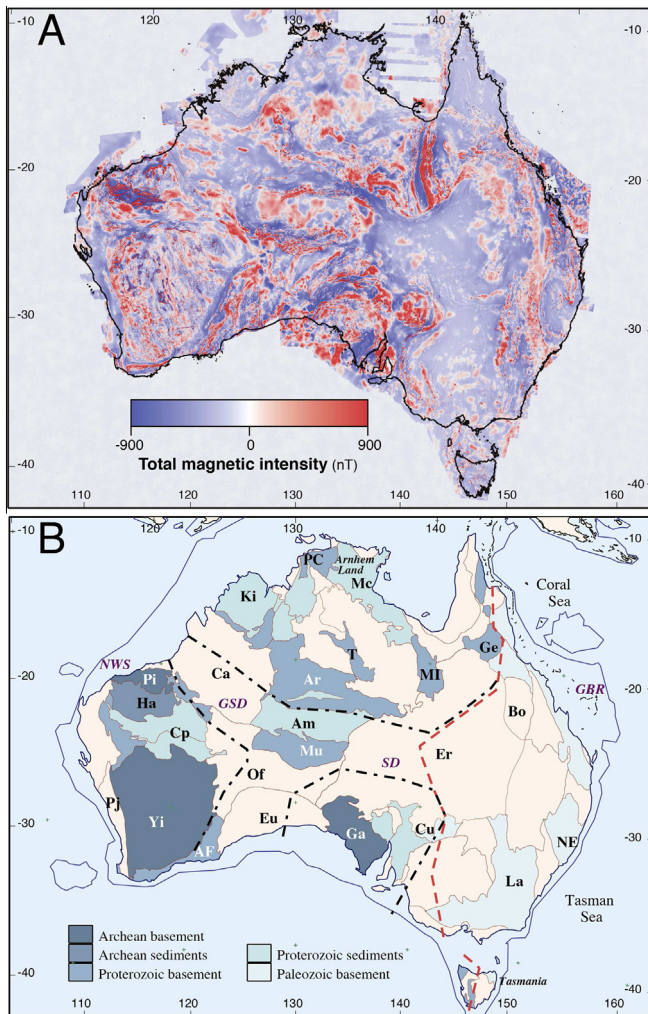
Fig. 2. (A) Magnetic anomaly map of Australia. These data are based on the published magnetic anomaly data [10], and are then projected, reduced to the pole using a variable reduction to the pole algorithm, and the spectral averaging technique described in Fig. 4. (B) Simplified relationships of major tectonic features of Australia. The chain dotted lines represent the margins of major cratons ([11], and modified with reference to recently acquired seismic reflection lines). The red dashed line represents an approximate surface boundary between Precambrian outcrop in the west and central areas of Australia, and the Phanerozoic east side of Australia (after [12]; modified with reference to seismic reflection lines acquired subsequently to this publication). Marked features: AF: AlbanyFraser Orogen, Ar: Arunta Block, Am: Amadeus Basin, Ca: Canning Basin, Co: Cooper Basin, Cp: Capricorn Orogen, Cu: Curnamona Craton, Er: Eromanga Basin, Eu: Eucla Basin, Ga: Gawler Craton, Ge: Georgetown Inlier, Ha: Hamersley Basin, Ki: Kimberley block, La: Lachlan Orogen, Mc: MacArthur Basin, MI: Mt Isa Inlier, Mu: Musgrave Orogen, NE: New England Orogen, Of: Officer Basin, PC: Pine Creek Inlier, Pi: Pilbara Craton, Pj: Pinjarra Orogen, T: Tennant Creek Inlier, Yi: Yilgarn Craton; SD: Simpson Desert, GSD: Great Sandy Desert, GBR: Great Barrier Reef, NWS: North West Shelf.

Understanding the contacts between the major elements and geological provinces of Australia is crucial to unravelling the geological history of the continent in the absence of outcrop. The configuration of crustal provinces is also of prime interest to minerals and energy exploration of the continent. With many of the outcropping mineral deposits discovered, the search for new metallogenic provinces will continue at depth, underneath cover. The definition of the extent of known mineralising provinces as they continue undercover is a key component of such a search; the base of magnetisation can highlight these boundaries of provinces. Finally, using the base of magnetisation to infer the Curie depth also can provide constraints on temperature at depth, which is of interest for geothermal energy exploration [15].

Previous studies of the base of magnetisation or Curie depth across Australia have been limited. The base of magnetisation was mapped using an equivalent source layer model from satellite magnetic data [6]. Mayhew et al. [16] also used satellite magnetic data and forward modelling of a simple 2D magnetic model (with a depth to top and depth to base, and variable magnetic properties) to examine the Curie depth along a seismic traverse in the Archean Yilgarn Craton. This study established that the Curie depth was particularly deep for the eastern side of the Yilgarn, with the Curie depth into the mantle, but shallower on the western side of the craton. These results are consistent with the known heat flow data for the region [13,17]. A continental scale assessment of the Curie depth for Australia was also performed by Fox Maule et al. [18]. This work used the same constant susceptibility model with initial geometry from 3SMAC as used in the study of Antarctica by Fox Maule et al.[4], to extract equivalent-source dipoles in an inversion of satellite magnetic data. The results of [18] indicated a distinct difference in Curie depths between eastern and western Australia, with western Australia dominated by deeper Curie depths. The deepest Curie depths were inferred in the Northern Territory, beneath the onshore Carpentaria Basin and also in the region surrounding Mt Isa. The method used by Fox Maule et al. [18] assumes a constant average susceptibility to estimate the maximum depth of magnetisation and hence Curie depth. In regions of stronger magnetic susceptibility, such as the Hamersley Basin, this will tend to overestimate the Curie depth, and the converse will be true for areas with a lower than average magnetic susceptibility.

2. Methodology

In this study, we aim to establish the base of magnetisation of Australia, to rigorously analyse the analytic uncertainty inherent in the data we used, and to explore the potential for these results to constrain the Curie depth of Australia. We therefore need to adopt an approach that can be performed entirely automatically and is also relatively fast, to allow analysis of the uncertainty of the model results.
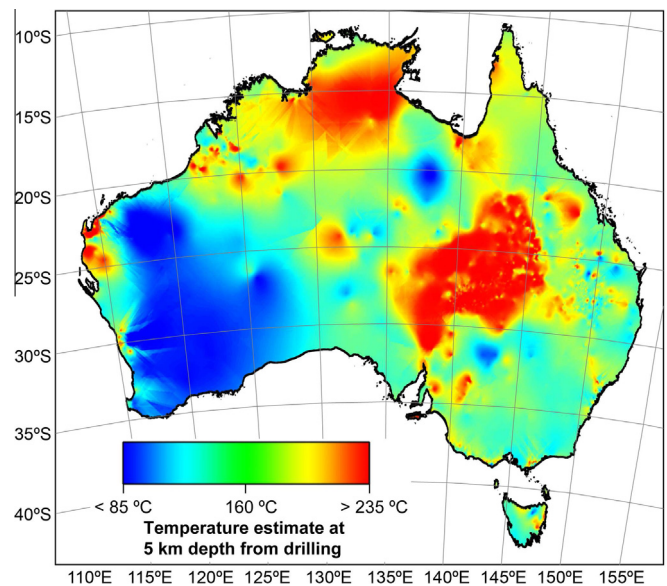
Fig. 3. Temperature at 5 km depth, as estimated by Gerner and Holgate [13]. This is extrapolated from temperature and heatflow measurements in 1500 drillholes across the Australian continent, and reflects the large variations in geothermal gradients and heat production.

We chose the approach used by Bouligand et al. [8], which is based on a one-dimensional, fractal model of magnetisation for the forward calculation. The natural logarithm of the radially averaged 1D power spectra of observed magnetic data ($\ln(1DPSD)$), observed at multiple wavenumbers k_h, can be expressed as an analytic relation between the depth to the top (z_t) and thickness (Δz) of a layer of randomly distributed but fractal magnetic sources, with the level of self-similarity of the fractal sources described by the parameter β. The relation depends on the modified Bessel function of the second kind K_α (N.B. for this forward model, $\alpha = \frac{1+\beta}{2}$), and the gamma function Γ, and where C is a constant (Eq. (1)).

$$
\begin{aligned}
\ln(1DPSD) = {} & C - 2k_h z_t - (\beta - 1)\ln(k_h) \\
& + \left[-k_h \Delta z + \ln\left(\frac{\sqrt{\pi}}{\Gamma\left(1 + \frac{\beta}{2}\right)} \left(\frac{\cosh(k_h \Delta z)}{2} \Gamma\left(\frac{1+\beta}{2}\right) \right. \right. \\
& \left. \left. - K_{\frac{1+\beta}{2}}(k_h \Delta z)\left(\frac{k_h \Delta z}{2}\right)^{\frac{1+\beta}{2}} \right) \right) \right]
\end{aligned}
$$

(1)

Note that this forward model contains no explicit assumptions about magnetic susceptibility.

We extract the power spectra for different parts of the continent from a processed version of the 5th edition of the magnetic anomaly map of Australia [10]. These magnetic anomalies are projected to an equal area projection and are also differentially reduced to the pole [19].

To extract the spatial wavenumber representation of the data required for the 1D power spectra, we use a novel procedure to stabilise the longest wavelength components of the continental magnetic anomaly dataset (Fig. 4). We use subsampling and averaging in the frequency domain, with an ensemble approach to derive multiple scale representations of the magnetic data. To reduce the data set to manageable proportions we subsample to 1.28 km sampling, equivalent to a 16-fold reduction. This gives a 4096×4096 dataset that can be directly transformed into the frequency domain with excessive computational resources. To achieve the 16-fold down-sample of the entire continental dataset, we make use of all the 256 possible versions derived by moving the sampling pixels in the north-south and east-west directions. Each of the realisations then has the 16-fold subsample but based on an independent set of sampled pixels. We then Fourier transform each of these spatially subsampled datasets to the spatial wavenumber domain and average the spatial Fourier components of the individual 256 realisations. We also invert back to the spatial domain to provide a stabilised dataset with local noise suppressed.

This approach not only stabilizes the resultant average spectrum, but also allows a measure of the standard deviations representing the spatial noise. The ensemble average retains the key spatial components to a higher degree of fidelity than simple subsampling.

For finer scale analysis we use successively halve windows across the continental data set, and use 64-fold, then 16-fold and finally 4-fold averaging for the spatial spectra at each step. In this way we achieve a stable representation of the longest wavelength features representable at each window scale, and a measure of the uncertainty of the 1D power spectra used for this analysis for the depth of magnetisation. The approach is similar, in principle, to the resolution pyramid approach for edge detection employed by Tanimoto and Pavlidis [20].

The stabilised magnetic anomaly data, at the finest scales of our subsampling procedure, are then tiled using an overlapping moving window of 400×400 km, with the window centre moved 60 km between different windows. This window width was chosen so that a relatively deep base of magnetisation could be mapped ([8] discuss the requirements for window widths). This hierarchical process produced 3600 windows of data. The data for each window are transformed into the frequency domain, and the 2D spatial power spectra are computed. The 2D spectra are then radially averaged to remove any directional effects in the 1D power spectra, and the natural logarithm is then applied to produce quantities suitable for comparison with the forward model.

We seek to extract information on the character of the sources of the magnetic field and their uncertainties from the suite of spectra constructed from the observations. We need to avoid dependence on any assumed initial conditions and so employ a nonlinear inversion procedure with a wide exploration of the available parameter space. There are a number of inverse techniques available to allow for the determination of uncertainty through a wide exploration of the search domain. For example, we could have implemented any number of random sampling strategies or a more directed nonlinear inversion such as the Neighbourhood Algorithm [21]. To ensure a rigorous evaluation of the uncertainty in our results, however, a uniform contracting grid search [22] was used, exploiting the power of modern high-performance computing. The search domain was contracted to minimum and maximum acceptable parameters using a two-stage process. Firstly, a reconnaissance search was performed over a broad domain. This broad search allowed limits for each of the parameters to be defined, which then sets the confines of a reduced domain over which a final search was made. The procedure is a simple algorithm to implement: the domain of interest is divided into a number of equally spaced samples, which then allows us to evenly sample the entire search domain. The starting domain of the grid search used the range for z_t of 0–12 km with 0.1 km increments, for the fractal parameter the range 0.1–5 with increments of 0.1, for the thickness of the magnetic layer z the range 0–160 km in 0.5 km increments and for the constant C the range −50 to +100 with increments of 1 These ranges were subsequently refined within the grid search. To allow post-inversion statistical analysis, all models that were consistent with the 1D power spectra (within the estimate of the data error) were stored to produce our inversion ensemble.

Rather than producing a single or a few models, our inversion produces an ensemble of tens of millions of models per individual window. Evaluating this ensemble of results also requires automated methods and a wide range of different products can be produced. The results that we display are a weighted average of the ensemble results for each individual data window. The weights employed in this average are the inverse of the misfit of each model to the radially averaged 1D power spectra; models that more adequately fit the data therefore have more importance, but there is input from all models that can adequately explain the observed data. Since depth uncertainties induce limited sensitivity for the largest depths to the base of magnetisation, our weighted ensemble will serve to produce the deepest estimates of the base of magnetisation. The final result is a map of the depth to the base of magnetisation and its uncertainty assembled from the results of the individual tiles (Figs. 5 and 6).

3. Results and discussion

The results for the depth to the base of magnetisation (Fig. 5) and the analytic uncertainty (measured as one standard deviation within our weighted ensemble) derived from our methodology (Fig. 6) highlight major changes in this depth across the Australian continent that are larger than the uncertainty estimates that we have extracted in our inversion process. The base of magnetisation depth varies across Australia ranges from 10 to 12 km
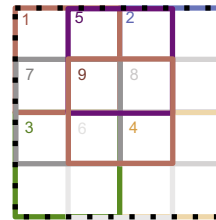
Process workflow
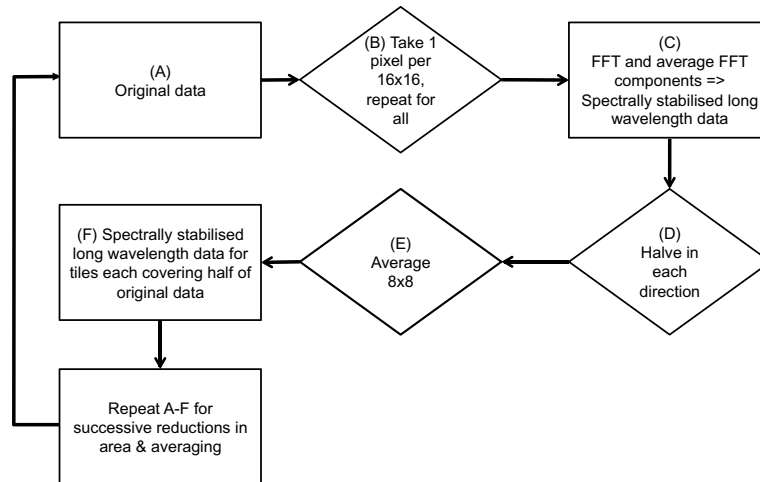
Data hierarchy
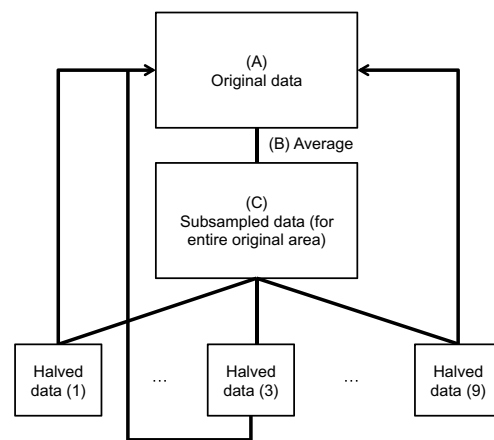

N.B. halving data:
yields 9 'half' areas

Fig. 4. Schematic representation of the procedures for generating ensemble averaged spatial spectra for the magnetic data. This process employs all available pixels once only in each realisation of the sub-sampled data set, and a stable spatial spectrum is extracted by the averaging of the spectra of the multiple sub-sampled versions. When the area is halved we achieve 9 realisations of possible zones of one quarter of the original data area. The ensemble averaging is then repeated for this lower level at a reduced window size to produce a successive layer in the hierarchy of spatial spectra. This process is repeated twice more to provide a full suite of area and scalelengths for which we have stable representations of the longest wavelength components in the original data.

beneath the Cooper Basin to as deep as 80 km beneath the Yilgarn Craton and other areas of Australia. The uncertainty determined from our inversion procedure, for most of Australia, is 7–10 km, as measured by the standard deviation of results in our ensemble. While this means that the depth to the base of magnetisation results are not as precise as would be required to evaluate minor features, it allows us reasonable certainty in interpreting broad-scale features. Our results are broadly consistent with both the known tectonic elements of Australia and the estimated temperature at 5 km (key anomalies from Fig. 3 reproduced on Fig. 8). Below, we will discuss these comparisons and use this to infer the Curie depth in areas of Australia; we will also discuss the deviations in the inferred Curie depth behaviour from expectations, and relations to other data.

In general, Archean and many Proterozoic cratons and provinces show the largest depths to the base of magnetisation in Australia in the range 55–80 km. These results are in agreement with the depth to the base of magnetisation being a proxy for the Curie depth in these regions; these long-lived cratons and provinces may be interpreted from our results as having relatively low geothermal gradients.

There is one exception to this result: the Pilbara Craton has a much shallower depth to the base of magnetisation than other Archean Cratons. The Pilbara Craton in our results has a depth to base of magnetisation of 20–30 km compared to up to 80 km depth in the Yilgarn Craton. This result may be explained by the fact that we may be mapping only the depth extent of magnetic minerals rather than the depth at which they have reached their Curie points. Furthermore, the very strong magnetic response of the Hamersley Basin, which contains significant iron ore deposits [23], may be masking a more subtle signal of the deepest magnetic sources which may well be less magnetic than this iron-rich basin. The Pilbara Craton is also the area with the most significant uncertainty in our inversion results, in the order of 15 km. The uncertainty is likely to be associated with the strength of the magnetisation of the region, which has the strongest magnetic intensity anomalies in the continent [10].

Geologically, the southern and eastern margins of the Archean Yilgarn Craton in the Albany-Fraser belt are well defined by our results. The eastern Yilgarn region is marked by rather a deep base of magnetisation (approx. 55 km), with a zone of slightly shallower depths running north-south in the centre of the craton. The deep
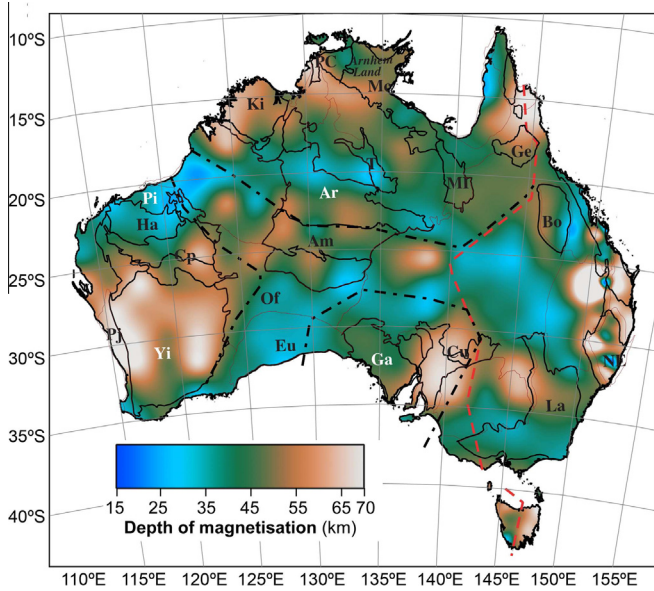
Fig. 5. Results of our inversion for the base of magnetisation/Curie depth of Australia. These results are a weighted result, where the depths of all models in our ensemble are weighted by the inverse of their data misfit. This weighting may bias to slightly deeper maximum depths of magnetisation. Tectonic provinces (Fig. 2B) are superimposed on our results to aid discussion.

base of magnetisation results that characterises the Yilgarn also extends to the east, underneath both the Albany-Fraser orogeny and the western side of the Eucla basin. These characteristic depths also continue up to the northeast and link to the Proterozoic Musgrave, Arunta and Warumpi provinces of the southern Northern Territory.

Large depths for the base of magnetisation also characterise the region around the Curnamona Province in western New South Wales and eastern South Australia, a resource-rich area containing ore deposits such as Broken Hill. The Gawler Craton, to the west of the Curnamona Province, is characterised by only moderate (40 km) depths to the base of magnetisation, which are restricted to the known outcrop of the core of the Gawler Craton [24]. The
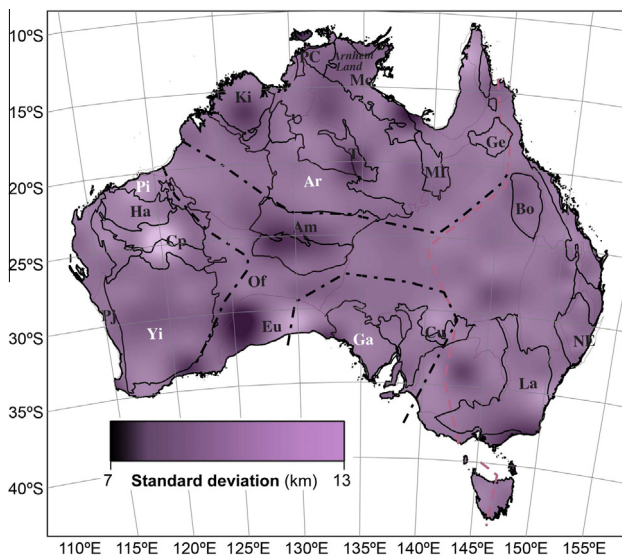
Fig. 6. Uncertainty expressed as one standard deviation of results after the weighting of all models in our inversion ensemble. Tectonic provinces (Fig. 2B) are superimposed on this figure to aid discussion.

areas surrounding the Gawler Craton to the north and the west feature shallower depths to base of magnetisation (up to 30 km) compared with the results observed for the craton itself.

The Adelaide Fold Belt/Flinders Ranges province, which is characterised by high concentrations of heat-producing elements and is known to have an elevated geothermal gradient [25] is not imaged as shallow depths to the base of magnetisation in our results, which would be expected if these results were mapping the Curie depth in this region. This is likely to be the result of both the window steps, which require a thermal anomaly to be significantly wider than 60 km in order to be visible, and also the large basic window size of 400 × 400 km which is needed to allow the imaging of deeper base of magnetisation results. In other words, the relatively narrow feature of the fold belt may be simply not be spatially resolvable. The large sampling window needed for accurate spectral analysis also has the potential of obscuring shallower features as the results are averaged over a large spatial area [8]. At the same time, our results may also indicate some complexity in the temperature regime at depths in the Adelaide Fold Belt: the heat flow may represent the partitioning of high-heat producing elements closer to the surface, and then there may significantly lower geothermal gradient at depth. More detailed studies, especially of thermal modelling in light of seismic reflection profiling results that bear on the distribution of the high-heat producing Neoproterozoic units [26], would be required to resolve this disagreement between our results and the observed thermal data near surface and in drillholes.

The relationships of our results to compilations of thermal estimates for the Australian continent highlight both areas where our depth to the base of magnetisation matches to expectations of Curie depth, and areas where it differs. Such differences may indicate areas where our understanding of the thermal regime is incomplete, or could arise from differences in geology resulting from processes such as major tectonic events changing magnetic mineralogy.

The shallowest depths to the base of magnetisation are beneath the Cooper basin in central Australia. This result is consistent with the drill hole data for this region where high temperatures are encountered at shallow depth ([13]: the spatially largest high temperature anomalies from these data are superimposed on our results in Fig. 7). The geothermal regime is reflected by the temperature estimate at 5 km.

Our results do not directly coincide with the mapping of the temperature anomalies for a number of reasons. Firstly, the spatial resolution of our data is, at best, 60 × 60 km the steps used in the movement of the sampling window that were chosen to attempt to balance resolution against computational power. Secondly, we see the influence of broad thermal anomalies away from any drilling control. As an example, there are limited constraints on the spatially largest temperature anomaly in the centre of Australia, beneath the Eromanga and other basins. Our results highlight a relatively large depth to the base of magnetisation extending to the east from the Arunta and Warumpi provinces beneath the Eromanga Basin. These deep results for the depth to base of magnetisation could imply a relatively cold region, highlighting the spatial extents of the Arunta and Warumpi provinces beneath the basin. The lower temperatures from the extension of the Arunta and Warumpi provinces is not sampled through drilling, so the colder region is not depicted in the results of [13].

The elevated temperature anomaly in northern Australia, beneath the onshore Carpentaria Basin, is also not reflected in our results. This anomaly is supported by limited drilling near uranium resources in the Northern Territory, and thus may represent an artefact of the interpolation method used for the OzTemp dataset [13]. This region contains significant reserves of uranium, such as the Ranger deposit [27]; however, these are confined to margins
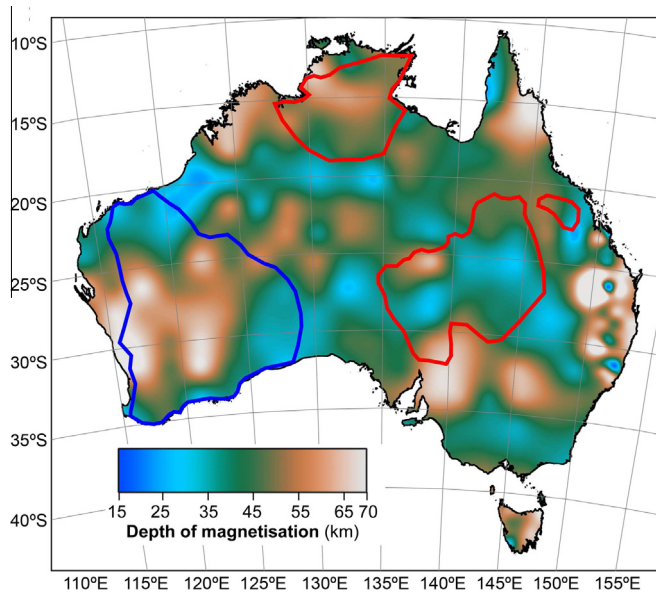
Fig. 7. Our results compared to key temperature anomalies in Australia ([13] and Fig. 3). The low temperature anomaly in the Yilgarn and Pilbara cratons is broadly supported by our results with generally deep Curie depths, implying a low geothermal gradient, in these areas. Likewise, the high temperature anomaly beneath the Eromanga Basin and the western Bowen Basin produces relatively shallow Curie depths. The high temperature anomaly beneath the onshore Carpentaria Basin in the north of Australia is not supported by our results, but this may represent limited constraints on the thermal anomalies in this region.

Fig. 8. Our results compared to the depth to Moho (from AusMoho: [30,31]). Blue colours represent where the Curie depth in our results is deeper than the Moho, and red colours represent where the Curie depth in our results is shallower than the Moho.

of the onshore Carpentaria Basin. With only limited deep drilling results from within the basin, the interpolation used to estimate the geothermal gradients away from these few observations is likely to have simply continued this anomaly beneath the basin. In consequence, the OzTemp results show a broad feature of elevated temperature.

As a final point of comparison with our results, we turn our attention to the relationship between our results and the crustal thickness of Australia. Some authors suggest that the Moho represents a lower boundary on magnetisation in continents due to changes in the mineralogy across the crust-mantle interface, although this relationship is not regarded as universal [28,29]. We have compared our results to a recent compilation of Moho depths for Australia ([30], as updated by Salmon et al. [31]) and find that there are large areas where the base of magnetisation lies beneath the Moho (Fig. 8).

In many cases, the differences between our results for the base of magnetisation and Moho are within the uncertainty of our results. However, in the case of the Yilgarn Craton of Western Australia, the base of magnetisation is significantly deeper than the Moho. The Moho is also significantly shallower than the base of magnetisation for both the Curnamona Craton and the eastern side of Australia, in areas such as the New England Orogen. The anomalous depth to the base of magnetisation for the New England Orogen might be an artefact of our data projection, since the relevant tiles centred over the orogeny have limited onshore data; equally well, it may represent an inherent difference in the distribution of magnetisation for this region.

Another area where the base of magnetisation is shallower than the Moho estimate is beneath the Eucla Basin, an area where seismic constraints have been very limited. Recent reflection profiling, conducted by Geoscience Australia and the Geological Survey of Western Australia – due to be publically released in 2015, suggests that the Moho depth may need to be increased slightly beneath this basin. For the Eucla region, our results are significantly shallower than for both the Yilgarn Craton to the west and the
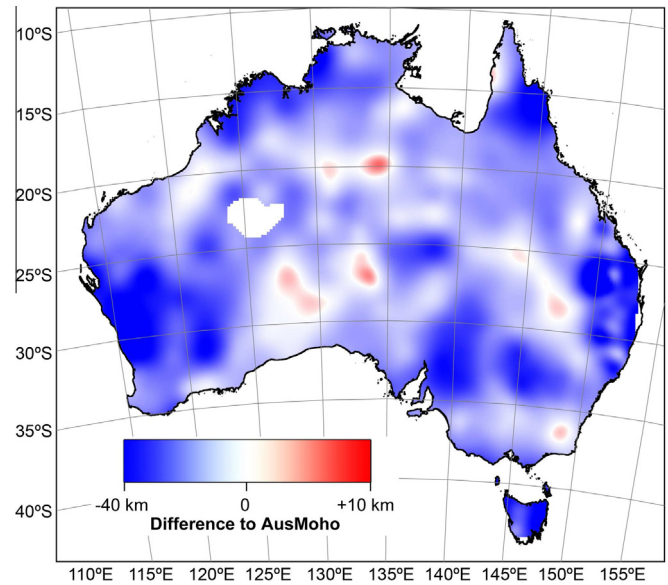
Gawler Craton to the east. Our Curie depth results, therefore, may be mapping a distinct province beneath this basin, which could help to explain the recent and preferential uplift of this region [32]. One such possible undercover province is the undercover extension of the Musgrave province, which has both anomalously thicker crust [33] and the potential for magnetic and radiogenic Proterozoic inclusions [34].

4. Conclusions

We have been able to define the base of magnetisation of Australia, and its related uncertainty, using high-performance computing. These results also allow us to interpret the Curie depth for the Australian continent with resolution to a horizontal scale of around 100 km. The uncertainty in our results is 7–10 km in depth, with the depth to the base of magnetisation ranging from 10 km in the warmest parts of Australia to 70 km for the coldest parts of the continent such as the Archean cratons. These results are in broad agreement with the estimated temperature at 5 km depth, although there are also differences, especially away from the regions with drill holes that provide most of the temperature constraints. Our results also have a good general correspondence with the surface geological provinces of Australia, and highlight that some of these provinces extend beneath younger cover. Examples are the distinctly deep base of magnetisation for the Warumpi, Arunta and Musgrave provinces that extends eastwards beneath the Eromanga Basin. Finally, our results also highlight previously unknown features, such as a distinctly shallower base of magnetisation beneath the Eucla basin which is not characteristic of either the Yilgarn Craton to its west, or the Gawler Craton to its west.

Acknowledgements

References

[1] Maus S, Gordon D, Fairhead D. Curie temperature depth estimation using a self-similar magnetization model. Geophys J Int 1997;129(1):163–8. http://dx.doi.org/10.1111/j.1365-246X.1997.tb00945.x.

[2] Telford W, Geldart L, Sheriff R. Applied geophysics. 2nd ed. Cambridge University Press; 1990.

[3] Artemieva I. The lithosphere: an interdisciplinary approach. 1st ed. Cambridge University Press; 2011.

[4] Fox Maule C, Purucker M, Olsen N, Mosegaard K. Heat flux in Antarctica revealed from satellite magnetic data. Science 2005;309(5733):464–7. http://dx.doi.org/10.1126/science.1106888.

[5] Spector A, Grant F. Statistical models for interpreting aeromagnetic data. Geophysics 1970;35(2):293–302. http://dx.doi.org/10.1190/1.1440092.

[6] Mayhew M, Johnson B. An equivalent layer magnetization model for Australia based on magsat data. Earth Planet Sci Lett 1987;83(1-4):167–74. http://dx.doi.org/10.1016/0012-821X(87)90060-4.

[7] Nataf H-C, Ricard Y. 3SMAC: an a priori tomographic model of the upper mantle based on geophysical modelling. Phys Earth Planet In 1996;95(1-2):101–22. http://dx.doi.org/10.1016/0031-9201(95)03105-7.

[8] Bouligand C, Glen J, Blakeley R. Mapping Curie temperature depth in the Western United States with a fractal model for crustal magnetization. J Geophys Res 2009;114:B11104. http://dx.doi.org/10.1029/2009JB006494.

[9] Kennett B, Blewett R. Lithospheric framework of Australia. Episodes 2012;35:9–22.

[10] Milligan P, Franklin R, Minty B, Richardson L, Percival P. Magnetic anomaly map of Australia. 5th ed. Canberra: Digital data, Geoscience Australia; 2010. https://www.ga.gov.au/products/servlet/controller?event=GEOCAT_DETAILS&catno=70282.

[11] Stewart A, Raymond O, Totterdell J, Zhang W, Gallagher R. Australian geological provinces. 2013.01th ed. Canberra, Australia: Geoscience Australia; 2013. http://www.ga.gov.au/metadata-gateway/metadata/record/gcat_c3fac1d5-48c1-624e-e044-00144fdd4fa6/Australian+Geological+Provinces.

[12] Direen N, Crawford A. The tasman line: where is it, what is it, and is it Australias Rodinian breakup boundary. Aust J Earth Sci 2003;50(4):491–502. http://dx.doi.org/10.1046/j.1440-0952.2003.01005.x.

[13] Gerner E, Holgate F. Oztemp interpreted temperature at 5 km depth. Canberra: Digital data, Geoscience Australia; 2010. GEOCAT reference 71143.

[14] Wyborn L, Wyborn D, Warren R, Drummond B. Proterozoic granite types in Australia: implications for lower crust composition, structure and evolution. Geol Soc Am Spec Paper 1992;272:201–10. http://dx.doi.org/10.1017/S0263593300007896.

[15] Okubo Y, Graf R, Hansen R, Ogawa K, Tsu H. Curie point depths of the island of Kyushu and surrounding areas, Japan. Geophysics 1985;53(3):481–94. http://dx.doi.org/10.1190/1.1441926.

[16] Mayhew M, Wasileski P, Johnson B. Crustal magnetization and temperature at depths beneath the Yilgarn block, Western Australia inferred from Magsat data. Earth Planet Sci Lett 1991;107(3-4):515–22. http://dx.doi.org/10.1016/0012-821X(91)90097-2.

[17] Cull J. An appraisal of Australian heat-flow data. BMR J Aust Geol Geophys 1982;7:11–21.

[18] Fox Maule C, Purucker M, Olsen N. Inferring magnetic crustal thickness and geothermal heat flux from crustal magnetic field models. Danish Climate Centre, Report 09–09. <http://core2.gsfc.nasa.gov/research/purucker/foxmaule_dkc09-09_greenland.pdf>; 2009.

[19] Cooper G, Cowan D. Differential reduction to the pole. Comput Geosci 2005;31(8):989–99. http://dx.doi.org/10.1016/j.cageo.2005.02.005.

[20] Tanimoto S, Pavlidis T. A hierarchical data structure for picture processing. Comput Graph Image Process 1975;42(2):104–19. http://dx.doi.org/10.1016/S0146-664X(75)80003-7.

[21] Sambridge M. Geophysical inversion with a Neighbourhood Algorithm I. Searching a parameter space. Geophys J Int 1999;138(2):479–94. http://dx.doi.org/10.1046/j.1365-246X.1999.00876.x.

[22] Hesterman J, Caucci L, Kupinski M, Barrett H, Furenlid L. Maximum-likelihood estimation with a contracting-grid search algorithm. IEEE Trans Nucl Sci 2010;57(3):1077–84. http://dx.doi.org/10.1109/TNS.2010.2045898.

[23] Huleatt M. Australian mines and mineral deposits selected commodities and operating status (1:5 000 000 scale map). Canberra, Australia: Geoscience Australia; 2010.

[24] Hand M, Reid A, Jagodzinski L. Tectonic framework and evolution of the Gawler Craton, South Australia. Econ Geol 2007;102(8):1377–95. http://dx.doi.org/10.2113/gsecongeo.102.8.1377.

[25] McLaren S, Sandiford M, Powell R, Neumann N, Woodhead J. Palaeozoic intraplate crustal anatexis in the mount painter province, South Australia: timing, thermal budgets and the role of crustal heat production. J Petrol 2006;47(12):2281–302. http://dx.doi.org/10.1093/petrology/egl044.

[26] Korsch R, Kositcin N. South Australian Seismic and MT workshop 2010: Extended abstracts, Geoscience Australia Record 2010/10. Canberra: Geoscience Australia. <http://www.ga.gov.au/corporate_data/70149/Rec2010_010.pdf>; 2010.

[27] Lally J, Bajwah Z. Uranium deposits of the Northern Territory, Northern Territory Geological Survey, Report 20, Darwin. Australia: Northern Territory; 2010. 87 p.

[28] Wasilewski P, Mayhew M. The Moho as a magnetic boundary revisited. Geophys Res Lett 1992;19(22):2259–62. http://dx.doi.org/10.1029/92GL01997.

[29] McEnroe S, Fabian K, Robinson P, Gaina C, Brown L. Crustal magnetism, lamellar magnetism, and rocks that remember. Elements 2009;5(4):241–6. http://dx.doi.org/10.2113/gselements.5.4.241.

[30] Kennett B, Salmon M, Saygin E, the AusMoho working group. AusMoho: the variation of Moho depth in Australia. Geophys J Int 2011;187(2):946–58. http://dx.doi.org/10.1111/j.1365-246X.2011.05194.x.

[31] Salmon M, Kennett B, Stern T, Aitken A. The Moho in Australia and New Zealand. Tectonophysics 2013;609:288–98. http://dx.doi.org/10.1016/j.tecto.2012.07.009.

[32] Sandiford M. The tilting continent: a new constraint on the dynamic topographic field in South-eastern Australia. Earth Planet Sci Lett 2007;261(1-2):152–63. http://dx.doi.org/10.1016/j.epsl.2007.06.023.

[33] Aitken A, Salmon M, Kennett B. Australias Moho: A test of the usefulness of gravity modelling for the determination of Moho depth. Tectonophysics 2013;609:468–79. http://dx.doi.org/10.1016/j.tecto.2012.06.049.

[34] Aitken A, Betts P. High-resolution aeromagnetic data over Central Australia assist Grenville-era (1300–1100 ma) Rodinia reconstructions. Geophys Res Lett 2008;35:1–6. http://dx.doi.org/10.1029/2007GL031563.